

Article

Assessing time series reversibility through permutation patterns

Massimiliano Zanin ^{1,2,*}, Alejandro Rodríguez González ¹, Ernestina Menasalvas Ruiz ¹ and David Papo ³

¹ Center for Biomedical Technology, Universidad Politécnica de Madrid, 28223 Pozuelo de Alarcón, Madrid, Spain.

² Department of Computer Science, Faculty of Science and Technology, Universidade Nova de Lisboa, 2829-516 Lisboa, Portugal.

³ University of Lille, 59800 Villeneuve d'Ascq, France.

* Correspondence: massimiliano.zanin@ctb.upm.es; Tel.: +34-91-336-4632

Version August 4, 2018 submitted to

Abstract: Time irreversibility, *i.e.* the lack of invariance of the statistical properties of a system under time reversal, is a fundamental property of all systems operating out of equilibrium. Time reversal symmetry is associated with important statistical and physical properties and is related to the predictability of the system generating the time series. Over the past fifteen years, various methods to quantify time irreversibility in time series have been proposed, but these can be computationally expensive. Here we propose a new method, based on permutation entropy, which is essentially parameter-free, temporally local, yields straightforward statistical tests, and has fast convergence properties. We apply this method to the study of financial time series, showing that stocks and indices present a rich irreversibility dynamics. We illustrate the comparative methodological advantages of our method with respect to a recently proposed method based on visibility graphs, and discuss the implications of our results for financial data analysis and interpretation.

Keywords: Time irreversibility; permutation entropy; visibility graphs; efficient market hypothesis.

1. Introduction

Time irreversibility is the lack of invariance of the statistical properties of a signal under the operation of time reversal. In other words, consider a time series describing the evolution of a system, $x(t)$ with $t \in [0, T]$ and its time reversal, *i.e.* the time series that would have been obtained had the system evolved in the opposite direction, or $x^{t,r}(t) = x(T - t)$. Irreversibility means that it is possible to find a characteristic that differs in the forward and backward versions, *i.e.* a function f calculated over the two time series such that $f(x^{t,r}) \neq f(x)$; or, in other words, that the observer can distinguish the forward, from the backward version of a given process. Note that the above definition does not impose any restriction on f .

Irreversibility can be due to the presence of memory, which acts as a hidden dissipative external force in a process [1] while the presence of noise results in a loss of irreversibility [2]. Thus, estimating the degree of irreversibility of a time series implicitly quantifies the degree of nonlinear dependences (memory), and therefore, the degree of time series predictability. Importantly, since linear Gaussian random processes and static nonlinear transformations of such processes are reversible, significant time irreversibility excludes Gaussian linear processes as models for the generating dynamics, implying instead nonlinear dynamics, non-Gaussian (linear or nonlinear), or linear ARMA models as possible generative processes [3–5].

The mere statistics of observed time series allows extracting information on the physics of the system under study. In particular, time reversal asymmetry provides information about the entropy production of the physical mechanism generating the series, even when the details of the underlying generating system are unknown [6]. Various methods to quantify time reversibility have been proposed and applied to the study of both biological and financial systems [2,7–14].

Here, we introduce a new method, based on permutation entropy [15,16] to evaluate irreversibility of time series at various temporal scales. With respect to existing methods, the proposed one presents various advantages: 1) it has no free parameters other than the embedding dimension of the permutation entropy; 2) as visibility graph methods [13] it is temporally local, and therefore allows assessing fluctuations; 3) assessing significance is straightforward, and does not rely on scaling arguments as visibility graph methods, over which it also has 4) a convergence speed advantage.

We first illustrate our method by evaluating the time irreversibility of a set of simple dynamical models, including stochastic models and chaotic dynamical systems, for which such property has theoretically been studied. We further show how the proposed approach can help elucidating the complex irreversibility dynamics of financial time series, representing 30 major European stocks and 12 world indices.

The time-reversal properties of financial time series allow testing the so-called efficient market hypothesis (EMH) [11]. The EMH asserts that financial markets are efficient with respect to an information set, *i.e.* that stocks incorporate all publicly available information useful in evaluating their prices and no single market agent can consistently outperform the market can be made from information based trading [17]. Importantly, efficiency is related to the amount of information available to predict future market prices, with lower efficiency corresponding to higher residual predictive information in the past sequence of stock prices [18]. The stringency of EMH's requirements suggests that no real market can ever be efficient *stricto sensu* [19] and that EMH should not be approached as an all-or-nothing property [20]. Various empirical studies have then undertaken to quantify the extent to which the EMH holds and, as a result to identify the sort of process governing market behaviour [20–23]. While financial series have been found to generally be time irreversible [2,7,11,24], it is possible to discriminate different degrees of such property. For instance, some stocks have been found to be more irreversible than others [14]. Likewise, emerging markets have been shown to be more time irreversible than developed ones, lending support to the relationship between efficiency and irreversibility [25].

We show that stocks' and indices' time series present a rich dynamics in terms of irreversibility. Specifically, while some time series may globally be reversible, they can become irreversible at specific temporal resolutions, *i.e.* when windows of specific length are considered. Additionally, such irreversibility may appear in a temporal localised way, suggesting that the dynamics of the element was somehow perturbed at that time.

The remainder of the paper is organised as follows. Firstly, the proposed method is described in Section 2; we also include a brief overview of the visibility graph (Section 2.3) and of the Markov chain (Section 2.4) approaches, as they will be used to benchmark our solution. We then validate the permutation patterns' method in synthetic (Section 3) and financial (Section 4) time series. Some conclusions are finally drawn in Section 5.

2. Assessing time series reversibility

2.1. Permutation patterns

The idea of analysing the permutation patterns present in a time series was initially introduced by Bandt and Pompe [15] to provide researchers with a simple and efficient tool to characterise the complexity of the dynamics of real systems. With respect to other approaches, as entropies, fractal dimensions, or Lyapunov exponents, it presents the advantage of being independent from any arbitrary thresholds or binning procedures [16]. For the sake of completeness, we here briefly review the process of calculating these permutation patterns.

Given a time series $X = \{x_t\}$, with $t = 1 \dots N$, this is usually divided in overlapping regions of length D , such that:

$$s \rightarrow (x_s, x_{s+\tau}, \dots, x_{s+\tau(D-2)}, x_{s+\tau(D-1)}). \quad (1)$$

81 D is called the *embedding dimension*, and controls the quantity of information included in each
82 region, while τ is the embedding delay. s further controls the beginning of each region, and thus the
83 degree of overlap between regions. Without loss of generality, in what follows we will consider $D = 3$
84 and $\tau = 1$.

85 The second step involves associating an ordinal pattern to each region. Values are sorted in
86 increasing order, and the ordinal pattern corresponding to the required permutation is saved for
87 further analysis. In other words, the permutation $\pi = (r_0, r_1, \dots, r_{D-1})$ of $(0, 1, \dots, D - 1)$ is defined
88 to fulfil:

$$x_{s+r_0} \leq x_{s+r_1} \leq \dots \leq x_{s+r_{D-2}} \leq x_{s+r_{D-1}}. \quad (2)$$

89 To illustrate, suppose a time series $X = (3, 2, 6, 4, 8)$. As $D = 3$, the first region would include
90 the values $(3, 2, 6)$, and the order required for sorting them is $(1, 0, 2)$ - that is, the second value is the
91 smallest, followed by the first and by the last. Similarly, the second region $(2, 6, 4)$ is associated with
92 the pattern $(0, 2, 1)$; and the third region $(6, 4, 8)$ with $(1, 0, 2)$.

93 2.2. Time reversibility of permutation patterns

94 After estimating all the permutation patterns in a time series, we analyse their frequency of
95 appearance, taking into account a time reversal process.

96 The total number of permutation patterns that may appear is given by $D!$. These patterns can be
97 paired together, such that each pattern composing a pair is the time reversal of the other. For instance,
98 for $D = 3$, six patterns are generated, which can pairwise be related as:

$$(0, 1, 2) \overset{\text{t.r.}}{\leftrightarrow} (2, 1, 0) \quad (3)$$

$$(1, 0, 2) \overset{\text{t.r.}}{\leftrightarrow} (2, 0, 1) \quad (4)$$

$$(1, 2, 0) \overset{\text{t.r.}}{\leftrightarrow} (0, 2, 1), \quad (5)$$

99 with $\overset{\text{t.r.}}{\leftrightarrow}$ representing a time reversal transformation.

100 In order to clarify this idea, let us consider the simple example of a time series resembling a
101 sawtooth, $X = (1, 2, 3, 1, 2, 3, 1)$. The series is stationary, as the average oscillates around 2.0, and five
102 permutation patterns of side $D = 3$ can be extracted: $(0, 1, 2)$, $(1, 2, 0)$, $(2, 0, 1)$, $(0, 1, 2)$ and $(1, 2, 0)$. It
103 can be observed that the system has a non-trivial dynamics, as it always increments in two consecutive
104 steps at the time - hence the upward pattern $(0, 1, 2)$. Let us now consider the time reversed series,
105 *i.e.* the same series observed from the end to the beginning: $X = (1, 3, 2, 1, 3, 2, 1)$. The new (time
106 reversed) permutation patterns are $(0, 2, 1)$, $(2, 1, 0)$, $(1, 0, 2)$, $(0, 2, 1)$ and $(2, 1, 0)$. As it should be
107 expected, the new time series can only diminish through the $(2, 1, 0)$ permutation pattern - which is, of
108 course, the time reversal equivalent of $(0, 1, 2)$. Note that this allows us to conclude that the time series
109 X is irreversible: if two consecutive increasing (respectively, decreasing) values are found, then we
110 can conclude that we are observing the direct (time reversed) time series, and we thus have a way of
111 defining a time directionality. This can further be generalised: a time series will be reversible if and
112 only if all permutation patterns composing the previous pairs appear with approximatively the same
113 frequency. This hypothesis will constitute the basis of the reversibility statistical test described below.

114 The value of $D = 3$ has here been chosen for the sake of clarity. While in principle larger values of
115 D may yield a richer description of the dynamics, this also results in the need of longer time series to
116 reach statistically significant results - both topics will be further discussed in the conclusions.

117 The previously defined pattern pairs and their frequency of appearance can be analysed in two
118 ways: in terms of the magnitude of the irreversibility, through the Kullback-Leibler divergence, and in
119 terms of its statistical significance, through a binomial test.

120 The irreversibility magnitude can be quantified by comparing two probability distributions,
 121 one represented by the probability of all patterns appearing in the direct (or original) time series,
 122 and a second one with the probabilities for the time-reversed time series. Following the previous
 123 example for $D = 3$, the first distribution is composed of the frequencies of patterns $\mathcal{P}_d =$
 124 $[p_{(0,1,2)}, p_{(2,1,0)}, p_{(1,0,2)}, p_{(2,0,1)}, p_{(1,2,0)}, p_{(0,2,1)}]$. As for the second distribution, it can be calculated by
 125 actually reversing the time series, or more simply by using the previous time reversal transformations -
 126 *i.e.* by considering the distribution $\mathcal{P}_r = [p_{(2,1,0)}, p_{(0,1,2)}, p_{(2,0,1)}, p_{(1,0,2)}, p_{(0,2,1)}, p_{(1,2,0)}]$. The difference
 127 between both distributions can then be estimated through the Kullback-Leibler divergence:

$$\mathcal{D}_{KL} = \sum_{i=1}^{D!} \mathcal{P}_d(i) \log \frac{\mathcal{P}_d(i)}{\mathcal{P}_r(i)}. \quad (6)$$

128 If the time series is perfectly reversible, the probabilities associated to patterns forming a pair
 129 should be the same, thus yielding a $\mathcal{D}_{KL} \approx 0$. On the other hand, the higher the value of \mathcal{D}_{KL} , the
 130 more irreversible the time series is. Note that \mathcal{D}_{KL} is not the only possibility for comparing the two
 131 distributions, being the Jensen-Shannon divergence a good alternative. While the latter presents the
 132 advantage of being symmetric, the former is commonly used in statistical physics [13,26]. Additionally,
 133 it has to be noted that Eq. 6 diverges when one or more permutation patterns are forbidden, *i.e.* their
 134 frequency is zero. This may happen when the time series under analysis is trivially irreversible (and
 135 possibly non-stationary), as is the case of a ramp function. This can easily be solved by adding a very
 136 small value to all probabilities, *i.e.*

$$\mathcal{D}_{KL} = \sum_{i=1}^{D!} \mathcal{P}_d(i) \log \frac{\mathcal{P}_d(i) + \epsilon}{\mathcal{P}_r(i) + \epsilon}, \quad (7)$$

137 such that $\epsilon \ll \min \mathcal{P}_d$ and $\epsilon \ll \min \mathcal{P}_r$. This situation is nevertheless seldom encountered in real
 138 time series, provided their length is large enough.

139 If the Kullback-Leibler divergence tells us the magnitude of the irreversibility of a time series, it
 140 yields little information about the statistical significance of the value. This problem can be solved by
 141 leveraging on the binomial nature of the patterns composing a pair. Specifically, if the time series
 142 is reversible, the number of times the two permutation patterns forming a pair appear should
 143 not statistically be different. Following the previous example, let us denote by $n_{(0,1,2)}$ and $n_{(2,1,0)}$
 144 respectively the number of times the patterns $(0, 1, 2)$ and $(2, 1, 0)$ have appeared; and let us define:

$$p = \frac{n_{(0,1,2)}}{n_{(0,1,2)} + n_{(2,1,0)}}. \quad (8)$$

145 The time series is not reversible if we can reject the null hypothesis that $p = 0.5$ in a two-sided
 146 binomial test. Note that the test should be repeated for all pairs of permutation patterns - three times
 147 in the case of $D = 3$.

148 One final discussion should here be added on the relationship between irreversibility and
 149 stationarity, and how such relationship affects the proposed methodology. On one hand, it is intuitive
 150 that a non-stationary process must also be irreversible - as a net change from state a to state b necessarily
 151 implies a time direction. Time irreversibility has therefore normally been assessed only in the presence
 152 of stationarity. On the other hand, it has recently been proposed that reversibility can be assessed even
 153 in non-stationary systems, by moving from a qualitative to a quantitative metric [26]. In the case of
 154 the methodology here proposed, the degree of irreversibility of a time series can be assessed by the
 155 magnitude of \mathcal{D}_{KL} (or of a Jensen-Shannon divergence), provided no permutation pattern is forbidden,
 156 *i.e.* $\mathcal{P}_r(i) > 0$ for all i . This quantitative aspect will be further explored in Section 4.

157 2.3. Directed Horizontal Visibility Graphs

158 One of the most recent and efficient ways of assessing the irreversibility of a time series is through
 159 the so-called directed Horizontal Visibility Graphs (dHVG). In what follows, this method is used for
 160 benchmark purposes, and, for the sake of completeness, is here briefly introduced.

161 From a general point of view, dHVG belong to a family of methods that map a time series into
 162 nodes of a network, based on geometric criteria [27,28]. In all of these methods, a complex network
 163 [29] is created, whose nodes correspond to the individual data of the time series; pairs of nodes are
 164 then connected when they fulfil some geometrical rule, usually based on whether one value can “see”
 165 the other one. In the specific case of dHVG, two nodes are connected if the line connecting both values
 166 is not obstructed by another intermediate point [28]. Mathematically, given two nodes i and j , a link is
 167 created if:

$$x_i, x_j > x_n, \forall n | i < n < j, \quad (9)$$

168 being x_i the element of the time series mapped into node i .

169 The resulting network can then be analysed using the wide set of tools provided by complex
 170 networks theory [30]. Of relevance for this work, the irreversibility of a time series can be assessed by
 171 comparing the distributions of in- and out-degrees (*i.e.* respectively the number of links arriving to
 172 and departing from a given node), and by calculating a Kullback-Leibler divergence [13,14]. Note that
 173 the in-degree of a node becomes its out-degree under a time reversal transformation. Therefore, for
 174 reversibility to hold both distributions ought to be equal, and the corresponding Kullback-Leibler
 175 divergence should converge to zero. For more details on the dHVG approach and the assessment of
 176 irreversibility, we refer the reader to the following studies [13,14,28].

177 2.4. Markov chain approach

178 We finally consider a classical method for detecting time series irreversibility, based on the
 179 representation of the underlying system as a Markov chain. In the case of a Markov chain with a
 180 transition matrix $P_{i,j}$ and steady-state distributions π_i , time symmetry implies $\pi_i P_{i,j} = \pi_j P_{j,i}$; a time
 181 series is then reversible if and only if $P_{i,j} = P_{j,i}$, for all i and $j \neq i$ [31]. We use this property to
 182 construct a simple test, which requires: *i*) binning the elements of the original time series into a set
 183 of bins (note that the number of bins is a parameter of the method); *ii*) calculate the transition matrix
 184 $P_{i,j}$; and *iii*) perform a binomial statistical test on each pair (i, j) , with $j \neq i$, to test the hypothesis that
 185 $P_{i,j} = P_{j,i}$.

186 3. Validation with synthetic time series

187 We validate the permutation patterns approach to irreversibility assessment, and compare it with
 188 the visibility graph one, through the application to a set of synthetic time series whose reversible or
 189 irreversible nature has already been studied theoretically. These are:

- 190 • Two reversible stochastic processes, namely a time series of values drawn from a Gaussian
 191 distribution $\mathcal{N}(0, 1)$, and an Ornstein-Uhlenbeck process, a mean-reverting linear Gaussian
 192 process T [32].
- 193 • Two dissipative chaotic maps, respectively a logistic map (defined as $x_{n+1} = ax_n(1 - x_n)$, with
 194 $a = 4.0$) and a Henon map ($x_{n+1} = 1 + y_n - ax_n^2$, $y_{n+1} = bx_n$, with $a = 1.4$ and $b = 0.3$).
 195 Dissipative systems are by definition irreversible [33].
- 196 • The Arnold Cat map, and example of a conservative chaotic map ($x_{n+1} = x_n + y_n$
 197 $\text{mod } (1)$, $y_{n+1} = x_n + 2y_n \text{ mod } (1)$). The analysed time series corresponds to the evolution
 198 of the x variable.
- 199 • The Lorenz chaotic system, defined as $\dot{x} = \sigma(y - x)$, $\dot{y} = x(\rho - z) - y$, and $\dot{z} = xy - \beta z$ (with
 200 $\rho = 28$, $\sigma = 10$ and $\beta = 8/3$, integration step of $dt = 0.01$). Unless otherwise stated, the analysed
 201 time series corresponds to the evolution of the x variable.

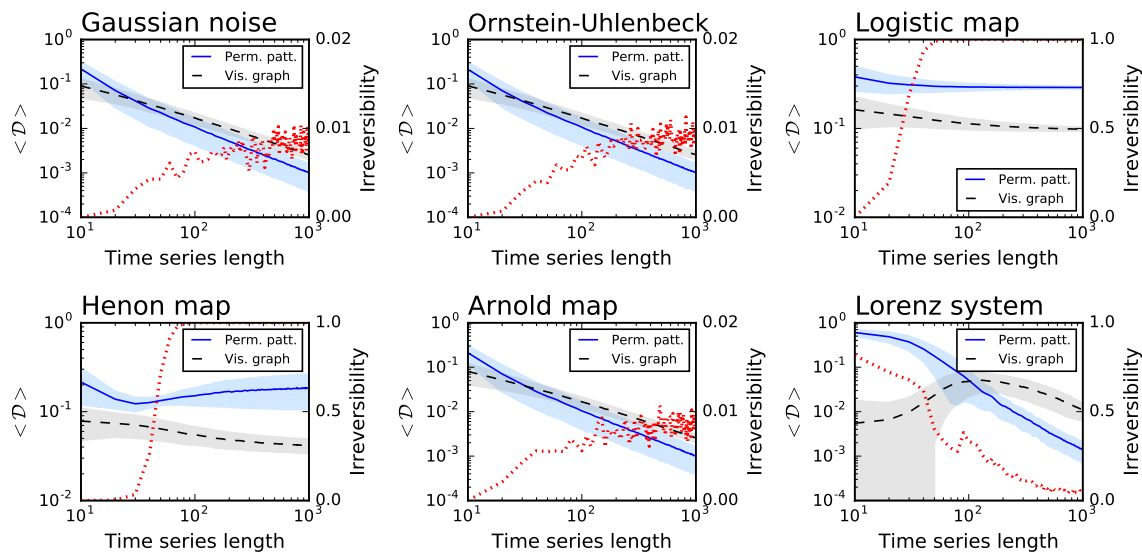


Figure 1. Irreversibility analysis of several synthetic dynamical models, as a function of the time series length. From left to right, top to bottom, the six panels represent Gaussian noise, an Ornstein-Uhlenbeck process, logistic, Henon and Arnold maps, and a Lorenz oscillator - see main text for details and parameters. In the left Y axis, the blue solid and black dashed lines respectively represent the average Kullback-Leibler divergence obtained by the permutation patterns and the visibility graph approach - note the blue and grey bands, depicting one standard deviation. On the right Y axis, the dotted red line indicates the fraction of simulations in which the time series is irreversible in a statistical significant way, with $\alpha = 0.01$.

202 For each of them, Fig. 1 reports: *i*) the average divergence \mathcal{D} yielded by the permutation patterns
 203 (blue line and one standard deviation band) and the visibility graph (black line and band) approaches;
 204 and *ii*) the fraction of times the time series is detected as irreversible by the permutation patterns
 205 approach in a statistical significant way (red dotted line, right Y axis, significance $\alpha = 0.01$). The two
 206 examples of stochastic processes and the Arnold map are recognised as irreversible in less than 1%
 207 of the realisations - as expected from the choice of a statistical significance level of $\alpha = 0.01$. On the
 208 other hand, the irreversibility frequency rapidly converges to one for the two dissipative chaotic maps
 209 - which are known to be irreversible [33]. Finally, a special situation can be observed for the Lorenz
 210 system: while its time series are mostly irreversible at short temporal scales, they become highly
 211 reversible when sufficiently long time windows are considered. To understand if such behaviour is a
 212 general property of the system, Fig. 2 Left reports the evolution of the irreversibility as a function of
 213 time series length, for the three channels of the Lorenz system. While the X and Y channels have a
 214 similar dynamics, the Z one is substantially different: first it is completely irreversible over long time
 215 scales, and second, the evolution of the irreversibility is not monotonic, with a minimum around 70
 216 and a peak every 60 time points. This abnormal behaviour for the Z time series is possibly due to its
 217 dynamics, which is well known to differ from those of the X and Y channels in terms of Lyapunov
 218 exponent [34] and autocorrelation (see Fig. 2 Right).

219 Fig. 1 further suggests that the permutation patterns approach to irreversibility can be more
 220 sensitive than the visibility graph one - note that the $\langle \mathcal{D} \rangle$ blue lines usually have a steeper slope, and
 221 converge faster than the black ones. Fig. 3 depicts the fraction of times the three considered methods
 222 detect that the underlying time series is irreversible in a statistical significant way ($\alpha = 0.01$), for very
 223 short time series lengths and for the two systems that were detected as irreversible (*i.e.* respectively
 224 the Logistic and the Henon maps). Note that, in order to calculate the statistical significance of the
 225 divergence yielded by the visibility graph approach, this has been compared with the ones obtained

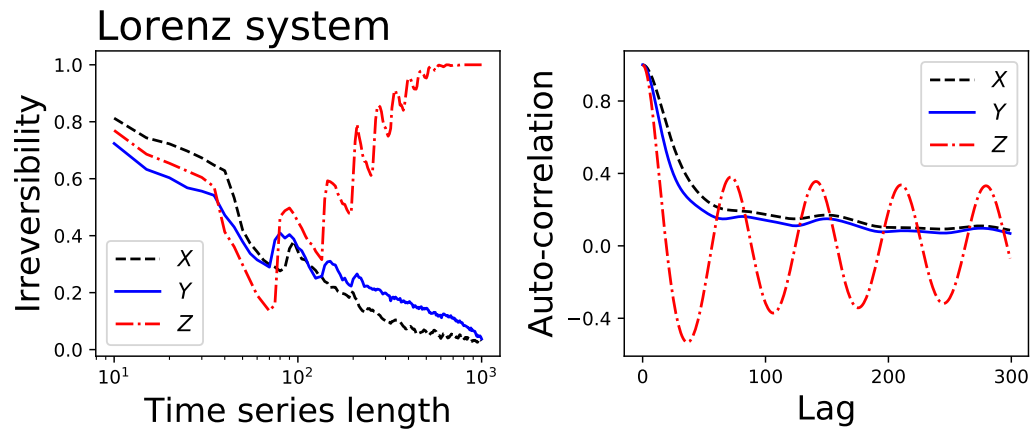


Figure 2. (Left) Fraction of irreversible time series yielded by a Lorenz chaotic system, as a function of the time series length. Black (dashed), blue (solid) and red (dash-dot) lines correspond respectively to the X, Y and Z channels of the system. (Right) Autocorrelation of the same three time series.

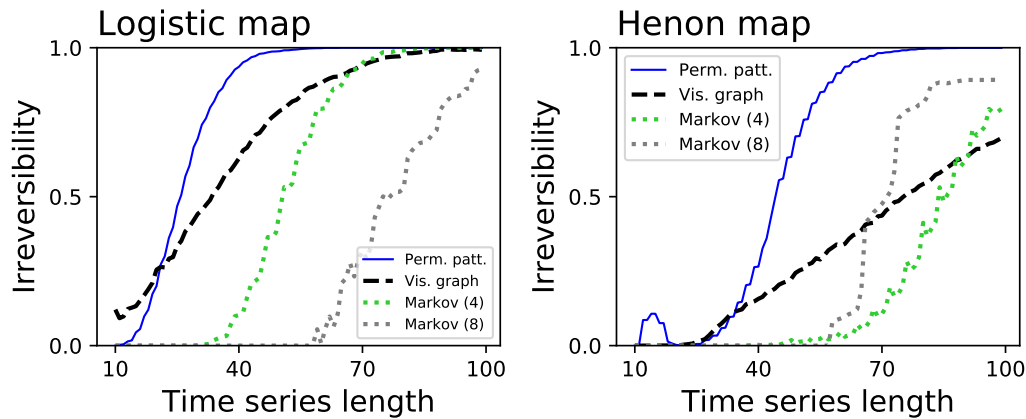


Figure 3. Analysis of the time series length required to reach a consistent irreversibility assessment. Both panels depict the fraction of times the permutation patterns (blue solid lines), the visibility graph algorithms (black dashed lines) and the Markov chain method (dotted lines) detect a statistically significant irreversibility, as a function of the time series length. Left and right panels respectively correspond to the logistic and Henon maps.

226 from randomly shuffled versions of the time series, and the probability of finding a larger \mathcal{D} in the
 227 random realisations expressed as a p -value. Fig. 3 indicates that the permutation pattern approach
 228 requires shorter time series to reach a consistent output, something that is particularly conspicuous in
 229 the case of the Henon map. Additionally, these results highlight the benefit associated to parameter-free
 230 methods. Specifically, the Markov chain method has been tested with two different numbers of bins,
 231 respectively 4 (green dotted lines) and 8 (grey dotted lines), yielding different results depending on
 232 the underlying dynamics. The fact that the proposed methodology required no parameter estimation
 233 or tuning thus becomes an important practical advantage.

234 Finally, Fig. 4 explores the resilience of the proposed method with respect to the presence of noise.
 235 Specifically, we consider the previously described logistic map, and added a Gaussian noise:

$$x_{n+1} = ax_n(1 - x_n) + \sigma\zeta, \quad (10)$$

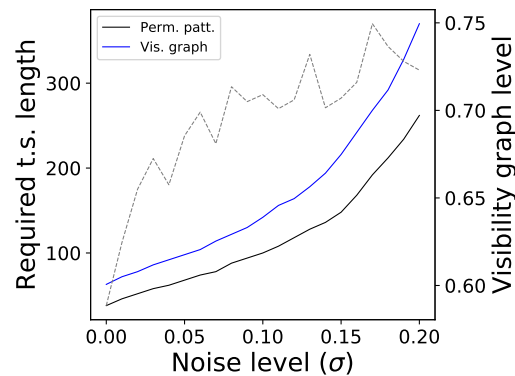


Figure 4. Resilience to noise. The two solid lines (left Y axis) depict the evolution of the time series length required to reach a 90% detection of irreversibility for the logistic map, according to the permutation patterns approach (black) and the visibility graph one (blue), as a function of the level noise. The dashed line (right Y axis) indicates the fraction of times the visibility graph method is detecting an irreversibility, when the permutation patterns method has reached a 90%.

236 with $a = 4.0$ and ξ being independent random numbers drawn from a Gaussian distribution
 237 $\mathcal{N}(0, 1)$. Note that noise is inherently reversible, and therefore its presence is expected to mask the
 238 irreversibility of the logistic map. We then measure the minimum time series length that allows to
 239 detect the irreversibility of the system the 90% of the times, and plot this as a function of the noise level
 240 σ . The two solid lines in Fig. 4 report the results, and indicate that the permutation patterns approach
 241 is more resilient than the visibility graph one.

242 Taken together, the numerical experiments carried out on synthetic time series indicate that the
 243 permutation patterns approach is comparable to the visibility graph one in assessing irreversibility.
 244 The former is nevertheless more sensitive, as it relies more on local patterns (of dimension D), and
 245 more resilient to noise, thus more suitable for the analysis of short time series. We will take advantage
 246 of this in Section 4, by analysing the temporal evolution of the irreversibility of real time series. Finally,
 247 the local nature of the permutation patterns approach makes it extremely computationally efficient
 248 - with a computational cost that scales linearly with the number of data points, as opposed to the
 249 quadratic growth of the visibility graph approach.

250 4. Application to financial time series

251 In order to further validate the proposed methodology, we assess the irreversibility of several
 252 financial time series. These can be thought of as relatively short realisations of complex stochastic
 253 processes whose dynamics is richer than most of the generated time series, and their characteristics
 254 (including reversibility) can change over time. Dynamical repertoire richness and time series shortness
 255 are two desirable aspects from a validation view-point. As previously introduced, if financial time
 256 series were shown to be irreversible, *i.e.* if some permutation patterns were favoured over their
 257 corresponding time-reversed counterparts, this would disprove the efficient market hypothesis (EMH)
 258 [11], as the asymmetry would be associated with information with which to improve the prediction of
 259 future prices.

260 We consider two sets of time series representing the daily evolution of, on one hand, the top-30
 261 European stocks by capitalisation; and, on the other hand, of 12 representative world stock market
 262 indices. Tabs. 1 and 2 report the two full lists, along with some basic characteristics. Both sets of time
 263 series have been obtained through Yahoo Finance, and include data from January 1st 2008 to January
 264 1st 2018 - note that the actual number of data points may differ, *e.g.* due to local bank holidays. In
 265 order to ensure the stationarity of all time series, the original values X_t have been transformed to
 266 $\hat{X}_t = \log_2 X_{t+1} / X_t$. The resulting series \hat{X} have been tested through an Augmented Dickey-Fuller unit

Table 1. List of the 30 considered stocks.

Stock code	Name	Country	Capitalisation
ABI.BR	Anheuser Busch Inbev NV	Belgium	182.039 B€
AI.PA	Air Liquide	France	46.635 B€
AIR.PA	Airbus SE	France	72.22 B€
ALV.DE	Allianz SE	Germany	91.67 B€
ASML.AS	ASML Holding N.V.	Netherlands	71.596 B€
BAYN.DE	Bayer AG	Germany	87.425 B€
BBVA.MC	Banco Bilbao Vizcaya Argentaria, S.A.	Spain	49.919 B€
BMW.DE	Bayerische Motoren Werke AG	Germany	62.545 B€
BN.PA	Danone SA	France	44.386 B€
BNP.PA	BNP Paribas SA	France	84.307 B€
CA.PA	Carrefour SA	France	14.13 B€
DBK.DE	Deutsche Bank AG	Germany	32.651 B€
DPW.DE	Deutsche Post AG	Germany	48.763 B€
DTE.DE	Deutsche Telekom AG	Germany	69.937 B€
EL.PA	Essilor International SA	France	24.22 B€
ENEL.MI	Enel SpA	Italy	53.528 B€
ENGL.PA	ENGIE SA	France	34.648 B€
ENI.MI	Eni S.p.A.	Italy	53.801 B€
FRE.DE	Fresenius SE & Co. KGaA	Germany	37.235 B€
G.MI	Assicurazioni Generali S.p.A.	Italy	25.281 B€
IBE.MC	Iberdrola, S.A.	Spain	42.207 B€
INGA.AS	ING Groep N.V.	Netherlands	64.689 B€
ITX.MC	Industria de Diseño Textil, S.A.	Spain	89.425 B€
MC.PA	LVMH Moët Hennessy Louis Vuitton S.E.	France	121.994 B€
OR.PA	L'Oréal S.A.	France	102.244 B€
ORA.PA	Orange S.A.	France	39.275 B€
PHIA.AS	Koninklijke Philips N.V.	Netherlands	31.07 B€
SAF.PA	Safran SA	France	37.748 B€
SAN.PA	Sanofi SA	France	87.918 B€
SU.PA	Schneider Electric S.E.	France	42.25 B€

Table 2. List of the 12 considered market indices.

Index code	Name	Country
BVSP	IBOVESPA	Brasil
DJI	Dow Jones Industrial Average	USA
FCHI	CAC 40	France
GDAXI	DAX	Germany
GSPC	S&P 500	USA
HSI	Hang Seng Index	Hong Kong
IXIC	NASDAQ Composite	USA
MERV	MERVAL Buenos Aires	Argentina
MXX	IPC Mexico	Mexico
N100	EURONEXT 100	Europe
N225	Nikkei 225	Japan
STOXX50E	EURO STOXX 50	Europe

267 root test [35], and for all of them the presence of a unit root was rejected in a statistically significant
 268 way (the larger p -value being $2.48 \cdot 10^{-14}$ for the BNP.PA stock).

269 Each time series was analysed in three different ways. The first one entails estimating global
 270 irreversibility, *i.e.* taking into account the whole time series. This corresponds to the irreversibility of
 271 the system, under the assumption that such property is stationary, or to the assessment of the average
 272 irreversibility. Three stocks and four indices resulted irreversible: respectively BBVA.MC, ENEL.MI,
 273 G.MI, and DJI, GDAXI, GSPC and IXIC. This indicates that markets have preferred ways (or patterns)
 274 when rallying up- or downwards, and are therefore strictly not efficient. It is also interesting to observe
 275 that irreversibility is more frequent in indices (four out of twelve) than in individual stocks; this may

276 suggest that irreversibility is a collective (or emergent) phenomenon, which is difficult to see in the
277 dynamics of individual elements, but shows up when considering groups of them.

278 Even when the complete time series is reversible, it is possible to find shorter sub-windows
279 which are not reversible in a statistically significant way. Thus, it may happen that time series are
280 globally reversible, but locally irreversible. We explore this possibility in a second analysis, in which
281 we extract all possible sub-windows of a given length from each time series, and calculate their average
282 irreversibility. Note that this allows estimating irreversibility as a function of the time window length,
283 and thus the relationship between irreversibility and time scales. In other words, this second approach
284 enables to study the local *vs.* global nature of irreversibility. Results of this analysis, in terms of the
285 fraction of windows yielding a statistically significant irreversibility ($\alpha = 0.01$) as a function of the
286 window length, are presented in Figs. 5 and 6. Three general patterns can be distinguished. First of
287 all, many time series that are globally reversible display noisy results, with very low irreversibility
288 probabilities, and usually around or below the significance threshold. Secondly, those time series that
289 are globally irreversible gain such properties at relatively long time scales - the evolution of the fraction
290 of irreversible windows constantly increases with the window size. Finally, some time series, which
291 are globally reversible, can contain irreversible windows with a significant probability; it thus seem
292 that, for those time series, irreversibility is a property confined to some specific time scales. This is the
293 case, for instance, of BAYN.DE (maximum of 20.12% for lengths of 225) or CA.PA (13.89% at 575).

294 Given that irreversibility is, in many cases, a localised effect, we finally checked whether different
295 stocks present a synchronised dynamics; *i.e.* if different stocks tend to become irreversible at the same
296 time. Fig. 7 presents a time map of the irreversibility of the 30 analysed stocks, when considering
297 windows of 200 data points. While irreversibility seems to be slightly more probable at the end of the
298 considered period, deviations from the expected value are not enough to support the hypothesis of a
299 synchronous dynamics.

300 5. Discussion and conclusion

301 We proposed a new method to quantify irreversibility in time series based on permutation entropy.
302 We tested our method on synthetic time series from various processes with known irreversibility
303 properties and on financial time series of stock prices and indices. For synthetic time series, the results
304 from our method are consistent with known irreversibility properties of the respective time series.
305 Remarkably, particularly for the Lorenz system, the method could detect non-trivial irreversibility
306 dynamics. Our results also show that while most financial time series are globally reversible, the
307 proposed method highlighted an interesting dynamics, with time windows in which the dynamics
308 was significantly irreversible. While the results from the permutation entropy-base method were in
309 line with those obtained with the dHVG-based method, see Fig. 8, the former method compared
310 favourably in terms of convergence speed, indicating that it can be more suitable for relatively short
311 time series. Additionally, the proposed method is able to better handle singular situations, provided
312 the modified version of Eq. 7 is used. For instance, it is able to detect the extreme irreversibility of a
313 ramp function; on the contrary, for such time series the dHVG-based method yields regular networks
314 with a constant degree of 1, as in both directions each value can only “see” the following one, thus
315 returning a \mathcal{D} of zero and wrongly suggesting a perfect reversibility.

316 Our results with synthetic time series are consistent with theoretical results, indicating that the
317 proposed method correctly identifies the underlying process. On the other hand, some results for
318 financial time series are somehow surprising. In particular, our method returned higher irreversibility
319 for some markets previously known to be among the most efficient ones (see Fig. 6). These results
320 were in good agreement with those obtained using dHVGs. Insofar as the presence of irreversibility
321 has been associated with violation of the EMH, our results suggest that permutation entropy-based
322 irreversibility and dHVGs may capture a dynamical feature that differs from standard measures of
323 market efficiency. Further investigations will need to clarify the reasons for this discrepancy as well as
324 the proper physical interpretation of these results and, more generally, of the methods’ significance.

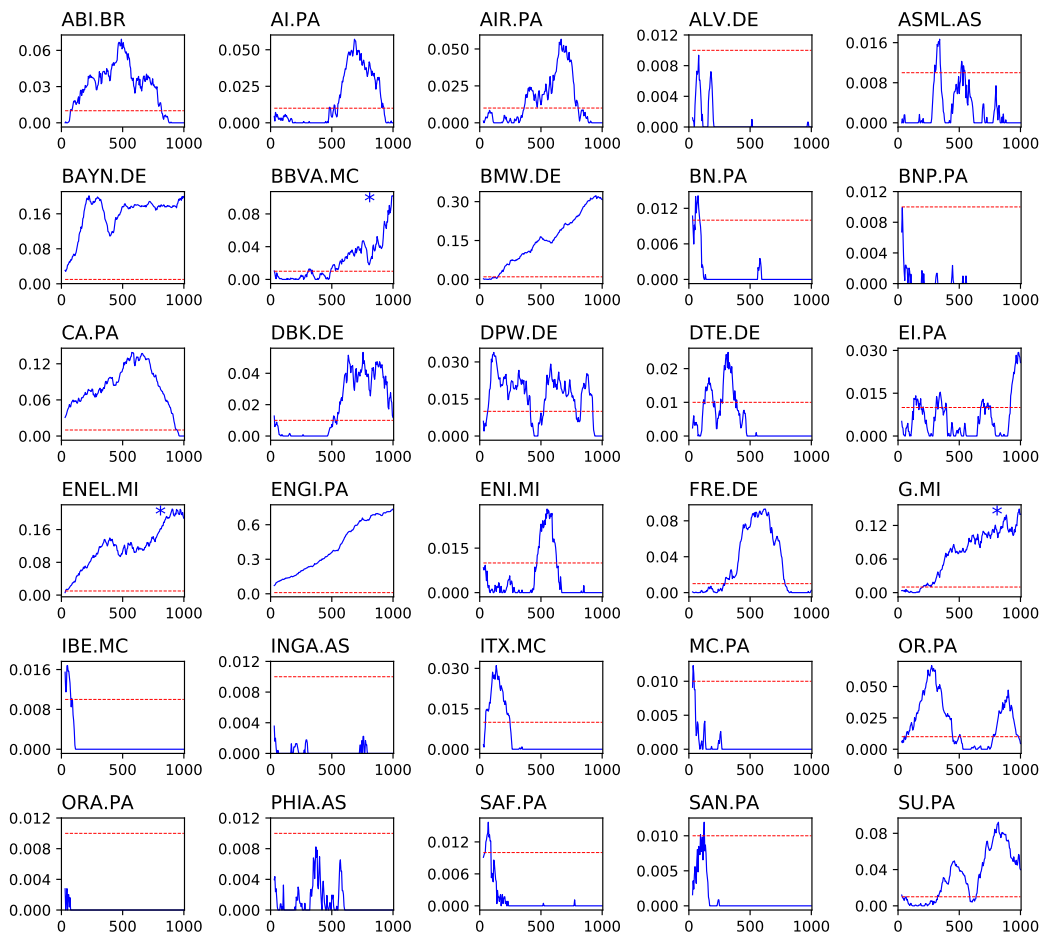


Figure 5. Reversibility of the 30 biggest European stocks by capitalization. The solid line of each panel depicts the fraction of windows in which the absence of reversibility was statistically significant ($\alpha = 0.01$), as a function of the window size. The horizontal dashed line represents the significance level of 0.01. An asterisk in the top right corner of a panel indicates that the stock is reversible when considering the whole time series.

325 One final note should be made on the choice of the embedding dimension D , which we set to
 326 $D = 3$ in this study. Using higher values of D increases the richness with which the dynamics of the
 327 system is captured - see [36] for an example. In addition, it has been shown that the permutation
 328 entropy (a closely related concept) is an approximation that converges to the true entropy rate of
 329 the system in the limit of increasing embedding dimension. It is thus logical to expect a similar
 330 behaviour for the proposed measure of reversibility, which may converge to a real value for large
 331 values of D . It is nevertheless important to take into account that increasing D also comes with several
 332 disadvantages. First, obtaining reliable statistics on the appearance of the permutation patterns and
 333 reducing the influence of random fluctuations requires longer time series - as a rule of thumb, it is
 334 usually recommended to have time series of length of at least $(D + 1)!$ [37]. This limits the resolution
 335 of the irreversibility analysis, and precludes detecting interesting phenomena at short time scales (as
 336 shown in Fig. 2). Second, although from a theoretical point of view, nothing precludes the use of
 337 higher embedding dimensions in the methodology proposed in this study, the computational cost
 338 scales exponentially with the embedding dimension - a limitation that may become serious when
 339 analysing large data sets as in some real-time applications.

340 **Author Contributions:** All authors developed the idea. MZ executed the numerical experiments and prepared
 341 the figures. All authors wrote and reviewed the manuscript.

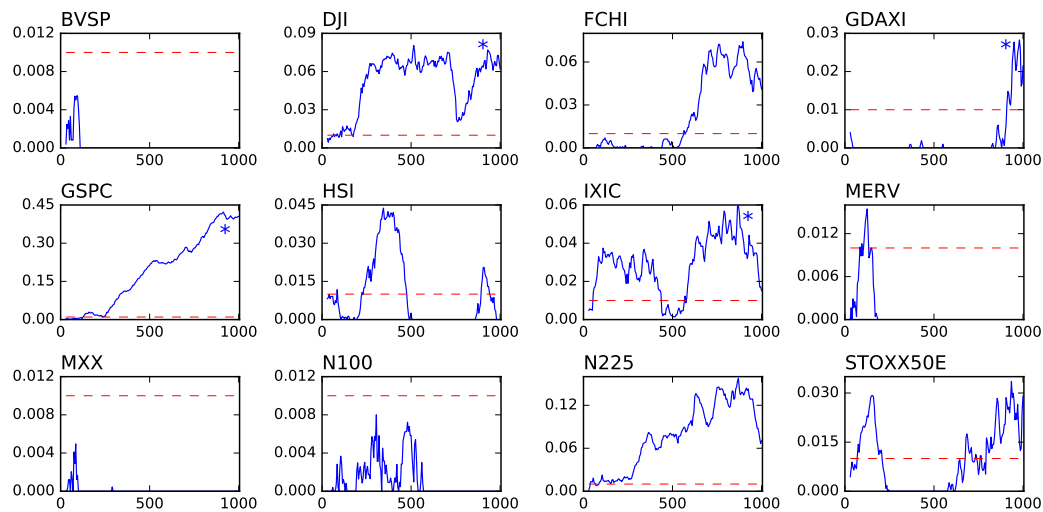


Figure 6. Reversibility of 12 market indices. The solid line of each panel depicts the fraction of windows in which the absence of reversibility was statistically significant ($\alpha = 0.01$), as a function of the window size. The meaning of the horizontal dashed lines and of the asterisks is the same as in Fig. 5.

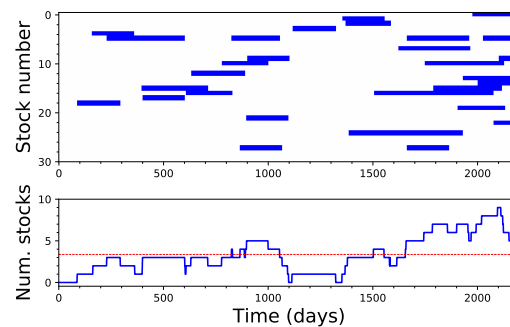


Figure 7. Analysis of the synchronicity between irreversible windows. The top panel depicts the time intervals when each stock time series is detected as irreversible, using windows of 200 data points. The bottom panel reports the evolution of the number of stocks that were irreversible at the same time. The dashed red line represents the expected number of irreversible stocks under the assumption of independence.

342 **Conflicts of Interest:** The authors declare no conflict of interest.

343

- 344 1. Puglisi, A.; Villamaina, D. Irreversible effects of memory. *EPL (Europhysics Letters)* **2009**, *88*, 30004.
 345 2. Xia, J.; Shang, P.; Wang, J.; Shi, W. Classifying of financial time series based on multiscale entropy and
 346 multiscale time irreversibility. *Physica A: Statistical Mechanics and Its Applications* **2014**, *400*, 151–158.
 347 3. Lawrance, A. Directionality and reversibility in time series. *International Statistical Review/Revue*
 348 *Internationale de Statistique* **1991**, pp. 67–79.
 349 4. Stone, L.; Landan, G.; May, R.M. Detecting time's arrow: a method for identifying nonlinearity and
 350 deterministic chaos in time-series data. *Proc. R. Soc. Lond. B. The Royal Society*, 1996, Vol. 263, pp.
 351 1509–1513.
 352 5. Cox, D.R.; Hand, D.; Herzberg, A. *Foundations of statistical inference, theoretical statistics, time series and*
 353 *stochastic processes*; Cambridge University Press, 2005.
 354 6. Roldán, É.; Parrondo, J.M. Estimating dissipation from single stationary trajectories. *Physical review letters*
 355 **2010**, *105*, 150607.

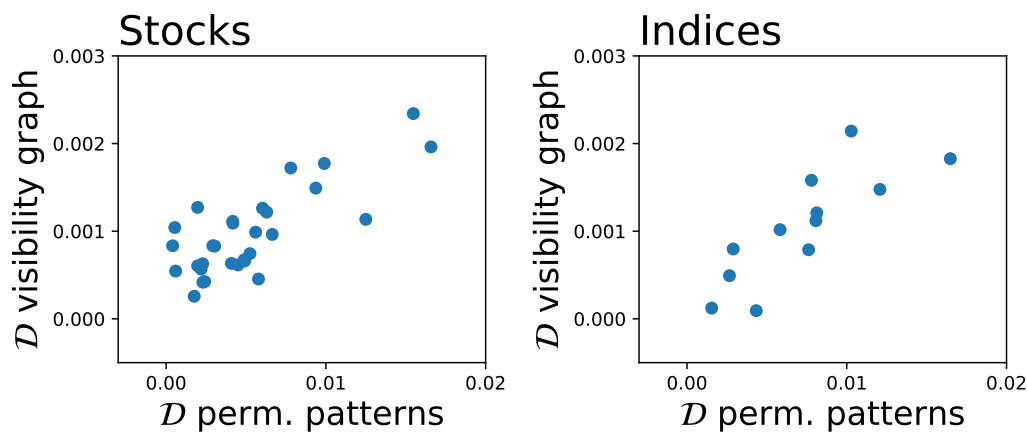


Figure 8. Analysis of the similarity of the irreversibility, as yielded by the proposed method and by the visibility graph approach. Left and right panels respectively correspond to stocks and indices time series.

- 356 7. Ramsey, J.B.; Rothman, P. Time irreversibility and business cycle asymmetry. *Journal of Money, Credit and*
 357 *Banking* **1996**, *28*, 1–21.
- 358 8. Daw, C.; Finney, C.; Kennel, M. Symbolic approach for measuring temporal “irreversibility”. *Physical*
 359 *Review E* **2000**, *62*, 1912.
- 360 9. Kennel, M.B. Testing time symmetry in time series using data compression dictionaries. *Physical Review E*
 361 **2004**, *69*, 056208.
- 362 10. Costa, M.; Goldberger, A.L.; Peng, C.K. Broken asymmetry of the human heartbeat: loss of time
 363 irreversibility in aging and disease. *Physical review letters* **2005**, *95*, 198102.
- 364 11. Zumbach, G. Time reversal invariance in finance. *Quantitative Finance* **2009**, *9*, 505–515.
- 365 12. Donges, J.F.; Donner, R.V.; Kurths, J. Testing time series irreversibility using complex network methods.
 366 *EPL (Europhysics Letters)* **2013**, *102*, 10004.
- 367 13. Lacasa, L.; Nunez, A.; Roldán, É.; Parrondo, J.M.; Luque, B. Time series irreversibility: a visibility graph
 368 approach. *The European Physical Journal B* **2012**, *85*, 217.
- 369 14. Flanagan, R.; Lacasa, L. Irreversibility of financial time series: a graph-theoretical approach. *Physics Letters*
 370 *A* **2016**, *380*, 1689–1697.
- 371 15. Bandt, C.; Pompe, B. Permutation entropy: a natural complexity measure for time series. *Physical review*
 372 *letters* **2002**, *88*, 174102.
- 373 16. Zanin, M.; Zunino, L.; Rosso, O.A.; Papo, D. Permutation entropy and its main biomedical and
 374 econophysics applications: a review. *Entropy* **2012**, *14*, 1553–1577.
- 375 17. Fama, E.F. Efficient capital markets: A review of theory and empirical work. *The journal of Finance* **1970**,
 376 *25*, 383–417.
- 377 18. Eom, C.; Oh, G.; Jung, W.S. Relationship between efficiency and predictability in stock price change.
 378 *Physica A: Statistical Mechanics and its Applications* **2008**, *387*, 5511–5517.
- 379 19. Campbell, J.Y.; Lo, A.W.C.; MacKinlay, A.C. *The econometrics of financial markets*; Vol. 2, princeton University
 380 press Princeton, NJ, 1997.
- 381 20. Lim, K.P. Ranking market efficiency for stock markets: A nonlinear perspective. *Physica A: Statistical*
 382 *Mechanics and its Applications* **2007**, *376*, 445–454.
- 383 21. Cajueiro, D.O.; Tabak, B.M. The Hurst exponent over time: testing the assertion that emerging markets are
 384 becoming more efficient. *Physica A: Statistical Mechanics and its Applications* **2004**, *336*, 521–537.
- 385 22. Barunik, J.; Kristoufek, L. On Hurst exponent estimation under heavy-tailed distributions. *Physica A:*
 386 *Statistical Mechanics and its Applications* **2010**, *389*, 3844–3855.
- 387 23. Wang, Y.; Liu, L.; Gu, R.; Cao, J.; Wang, H. Analysis of market efficiency for the Shanghai stock market
 388 over time. *Physica A: Statistical Mechanics and its Applications* **2010**, *389*, 1635–1642.

- 389 24. Fong, W.M. Time reversibility tests of volume–volatility dynamics for stock returns. *Economics Letters* **2003**,
390 81, 39–45.
- 391 25. Jiang, C.; Shang, P.; Shi, W. Multiscale multifractal time irreversibility analysis of stock markets. *Physica A:
392 Statistical Mechanics and its Applications* **2016**, 462, 492–507.
- 393 26. Lacasa, L.; Flanagan, R. Time reversibility from visibility graphs of nonstationary processes. *Physical
394 Review E* **2015**, 92, 022817.
- 395 27. Lacasa, L.; Luque, B.; Ballesteros, F.; Luque, J.; Nuno, J.C. From time series to complex networks: The
396 visibility graph. *Proceedings of the National Academy of Sciences* **2008**, 105, 4972–4975.
- 397 28. Luque, B.; Lacasa, L.; Ballesteros, F.; Luque, J. Horizontal visibility graphs: Exact results for random time
398 series. *Physical Review E* **2009**, 80, 046103.
- 399 29. Strogatz, S.H. Exploring complex networks. *nature* **2001**, 410, 268.
- 400 30. Costa, L.d.F.; Rodrigues, F.A.; Travieso, G.; Villas Boas, P.R. Characterization of complex networks: A
401 survey of measurements. *Advances in physics* **2007**, 56, 167–242.
- 402 31. Norris, J.R. *Markov chains*; Number 2, Cambridge university press, 1998.
- 403 32. Weiss, G. Time-reversibility of linear stochastic processes. *Journal of Applied Probability* **1975**, 12, 831–836.
- 404 33. Mori, H.; Kuramoto, Y. *Dissipative structures and chaos*; Springer Science & Business Media, 2013.
- 405 34. Wolf, A.; Swift, J.B.; Swinney, H.L.; Vastano, J.A. Determining Lyapunov exponents from a time series.
406 *Physica D: Nonlinear Phenomena* **1985**, 16, 285–317.
- 407 35. MacKinnon, J.G. Approximate asymptotic distribution functions for unit-root and cointegration tests.
408 *Journal of Business & Economic Statistics* **1994**, 12, 167–176.
- 409 36. Bian, C.; Qin, C.; Ma, Q.D.; Shen, Q. Modified permutation-entropy analysis of heartbeat dynamics.
410 *Physical Review E* **2012**, 85, 021906.
- 411 37. Amigó, J.M.; Zambrano, S.; Sanjuán, M.A. True and false forbidden patterns in deterministic and random
412 dynamics. *EPL (Europhysics Letters)* **2007**, 79, 50001.